IOP Conf. Series: Journal of Physics: Conf. Series **821** (2017) 012027 doi:10.1088/1742-6596/821/1/012027

Preliminary design of a supercritical CO_2 wind tunnel

B Re[1], A Rurale[2], A. Spinelli[2] and A. Guardone[1]

[1] Department of Aerospace Science and Technology, Politecnico di Milano
Via La Masa 34, 20156, Milano, Italy
[2] Department of Energy, Politecnico di Milano, Via Lambruschini 4, 20156, Milano, Italy

E-mail: alberto.guardone@polimi.it

Abstract. The preliminary design of a test-rig for non-ideal compressible-fluid flows of carbon dioxide is presented. The test-rig is conceived to investigate supersonic flows that are relevant to the study of non-ideal compressible-fluid flows in the close proximity of the critical point and of the liquid-vapor saturation curve, to the investigation of drop nucleation in compressors operating with supercritical carbon dioxide and and to the study of flow conditions similar to those encountered in turbines for Organic Rankine Cycle applications. Three different configurations are presented and examined: a batch-operating test-rig, a closed-loop Brayton cycle and a closed-loop Rankine cycle. The latter is preferred for its versatility and for economic reasons. A preliminary design of the main components is reported, including the heat exchangers, the chiller, the pumps and the test section.

1. Introduction

Supercritical carbon dioxide (sCO_2) is currently being considered as working fluid in several industrial and power generation applications thanks to its relatively low critical pressure and its low critical temperature. The seminal work of Angelino and Feher points out the advantages of using sCO_2 for power generation [1, 2]. Indeed, sCO_2 Brayton power cycles can be used to exploit solar, geothermal and waste heat thermal sources. Advantages over e.g. steam include compactness of turbomachinery and high thermal efficiency at low temperature. Moreover, fewer corrosion issues may be encountered except than at high temperatures and pressures [3]. For nuclear power generation, sCO2 is preferred over steam for safety reasons in sodium cooled fast reactions [4]. Rapid expansion of supercritical solutions (RESS) of CO_2 is used in the chemical, pharmaceutical and food industry for particle generation or extraction of chemicals, see [5, 6, 7] and reference therein. Other applications include sterilization and cleaning [8].

The fluid dynamics of sCO_2 flows departs significantly from the well-known gas dynamics of dilute gases, such as air in standard conditions. For example, a relatively low speed of sound is observed at very high, liquid-like densities. Moreover, non-equilibrium shock structure is possibly observed due to the relaxation of the internal vibrational modes [9, 10]. In the supercritical and close-to-critical region, the heat transfer as well exhibits peculiar behavior [11, 12].

The dynamics of compressible fluids in the close proximity of the vapor-liquid saturation curve and critical point or within the supercritical region are referred to in the following as Non-Ideal Compressible-Fluid Dynamics (NICFD).

Despite its widespread usage, a comprehensive understanding of the fundamental properties of CO_2 flows in supercritical conditions is not available, yet. Preliminary theoretical and numerical studies using accurate equations of state [13] and non-ideal flow solvers [14, 15], are yet to

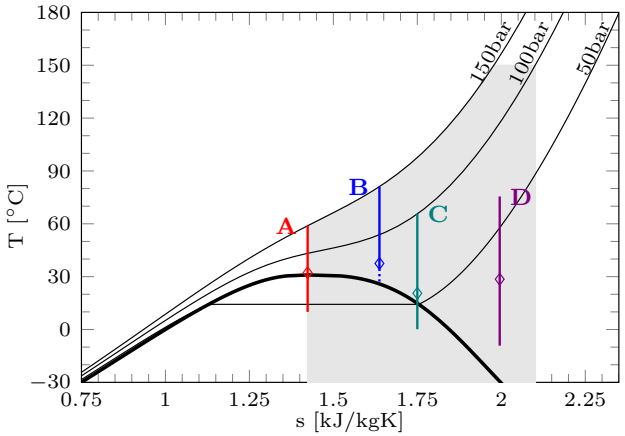

Figure 1: Thermodynamic plane temperature-entropy (T-s) with the four exemplary supersonic expansions to be realized in the SCO_2PRI facility. The region of interest (gray area), the saturation curve and three isobars are also reported. The symbol ◊ indicates the throat section, at $M = 1$.

be complemented with experimental data. Indeed, only recently experimental activities are being carried out to investigate the fundamentals of sCO_2 flows in supercritical conditions. For instance, Lettieri and collaborators at MIT assessed the condensation effects in sCO_2 compressors and defined a criterion to predict fluid condensation [16]. At KAIST, Lee's research team is developing an experimental facility to accurately take into account non-ideal gas effects during sCO_2 compressor design and performance analysis [17]. Finally, the university of Seville and Altran have designed a pressurized sCO_2 wind tunnel to improve the design of blade cascade of turbomachinery [18]. Diverse technology demonstrators of Brayton power cycles using sCO_2 are currently in operation in the USA [19, 20, 21], though the technology is not sufficiently developed to commercial exploitation [22]. For instance, heat transfer in sCO_2 cycles still raises some questions and requires further investigations to efficiently design heat exchangers [23, 24].

The design of a novel sCO_2 wind tunnel, named SCO_2PRI (Supercritical CO_2 for the PRocess Industry), is currently under-way at the CREA (Compressible-fluid dynamics for Renewable Energy Application) Laboratory of Politecnico di Milano. Fundamental studies of supersonic sCO_2 flows will be carried out in the close proximity of the critical point and the liquid-vapor saturation curve, where sCO_2 compressors for power production are designed to operate. Moreover, the test-rig will be used as a calibration tunnel for non-ideal flows pressure probes and optical measurement techniques, including Schlieren and Laser Doppler Velocimetry (LDV).

The present work outlines the preliminary design of the plant and the technical specifications of the relevant components. To attain supersonic speeds, the test section consists in a convergent-divergent nozzle followed by a rectangular-section chamber for flow visualization. Three possible configurations are initially taken into account to drive the fluid through the nozzle: an open-loop batch-operating system, an "inverse" Joule-Brayton cycle and a Rankine cycle. A preliminary analysis indicates that the last configuration is the most suitable for the operating conditions of interest. Then, the main components of the plant, namely the pump, the heater, the chiller and the heat exchangers are designed and a preliminary cost analysis is also carried out.

The present paper is structured as follows. In Section 2, the region of interest for the experimental observation of sCO_2 flows is determined, including conditions suitable for studying critical-point flows and condensing flows in compressors. The design constraints are also reported. The diverse test-rig configurations are presented and discussed in Section 3. The preliminary design of the main components of the chosen configuration, namely, closed-loop Rankine cycle, is reported in Section 4. In Section 5, final comments are given.

2. Region of interest and design constraints

The preliminary design of the SCO_2PRI test-rig starts with the definition of the thermodynamic region to be investigated, according to the relevant research and industrial applications of sCO_2

reported in the previous section.

Figure 1 depicts this region in the thermodynamic plane T-s, where T is the temperature and s is the specific entropy. Since the research interest is limited to NICFD flows, a first parameter taken into account to define the region of interest is the compressibility factor $Z = Pv/RT$, where v is the specific volume, P is the pressure and R is the gas constant. This quantity allows to estimate the deviation of the actual thermodynamic behavior from the ideal gas model, which predicts $Z \equiv 1$ [25]. Therefore, the region of interest is limited towards the vapor state by a maximum value of Z around $0.8 \div 0.85$. On the opposite side, it extends to the critical point. Moreover, the maximum pressure and temperature of $P_{\max} = 150$ bar and $T_{\max} = 150°\text{C}$ are imposed as design constraints, to limit the cost of the test-rig. The lowest temperature is arbitrarily fixed at $-30°\text{C}$ to include also a portion of the two-phase region, below the Vapor-Liquid Equilibrium (VLE) curve.

Within the region of interest, four exemplary isentropic expansions are defined and a convergent-divergent nozzle is adopted to reach supersonic speeds. The four expansions, labeled A, B, C and D, are depicted in the plane T-s in Figure 1. Initial computations of thermodynamic states are performed by means of the quasi-one-dimensional theory, which describes a steady, one-dimensional and isentropic flow in a duct neglecting viscous and thermal effects [26]. Thanks to this theory, it is possible to predict the inviscid core of the flow.

Expansion A starts at the maximum pressure $P = 150$ bar, it crosses the critical point and eventually ends inside the two-phase region. This expansion is probably the most challenging from the point of view of the control. At the exit of the nozzle, the pressure $P = 45$ bar is imposed, corresponding to a Mach number $M = 1.72$. The measurement of thermodynamic properties along the expansion process, and possibly in the close proximity of the critical point, would give a significant improvement in the fundamental knowledge of sCO_2 behavior in the NICFD regime. The second expansion (B) occurs completely in the supercritical region, starting from the maximum pressure of 150 bar down to 75 bar, namely to an isobar just above the critical one. The initial temperature is 81.1°C, so that a slightly supersonic expansion can be realized (exit Mach $M = 1.05$) and the compressibility factor at the nozzle inlet and outlet is around 0.5. Measurements of the fluid states through expansion B are relevant for investigating sCO_2 transport properties, for validating of CFD models and for assessing the isentropic expansion coefficient in non-ideal conditions. Finally, conditions that typically occurs in turbo-machinery are reproduced in expansions C and D. Condition C replicates the expansions that may occur in sCO_2 compressors near the leading edge of the impeller, which were investigated also by Lettieri et al. [16]. In this case, the design exit Mach number is $M = 1.49$. The fourth expansion (D) is representative, in terms of reduced conditions, of flows in Organic Rankine Cycle (ORC) turbine. The experimental investigation of this kind of flows is typically challenging because of the high temperatures, which might be close to the thermal stability limit of the fluid. However, the behavior of the organic fluid under consideration can be reproduced by an other fluid with a similar compressibility factor at the critical point, provided that their behaviors can be described by the same equation of state. Indeed, according to the principle of corresponding states, all fluids behave alike at the same thermodynamic conditions made dimensionless with respect to the critical-point values [25]. Thus, a flow of sCO_2 can reproduce, for instance, a siloxane flow in an ORC turbine in terms of reduced conditions at a lower temperature, which allows to measure more easily quantities of interest. In expansion D, the initial and final pressures are 62.1 and 20 bar, while the exit Mach number is $M = 1.42$.

To realize the outlined goal expansions, a plant suitable for feeding the converging-diverging nozzle has to be designed. The plant can possibly operate in a continuous fashion or as a batch facility, provided that the test time is sufficient to perform quasi-steady measurements. In this regard, some observations can be drawn according to the peculiar aim and scope of the test-rig. First, the SCO_2PRI is a research facility that is expected to operate discontinuously

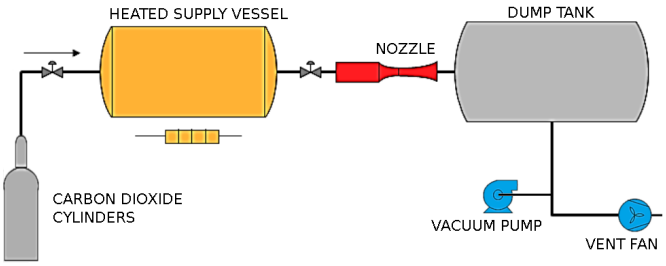

Figure 2: Sketch of the batch operating test-rig. A heated vessel, filled by CO_2 cylinders, discharges the fluid at supersonic speeds through a convergent-divergent nozzle into a low pressure tank.

Table 1: Test durations and mass discharged in batch-operating plant for expansion B. Results are reported for two throats (th) and three vessels (ves).

$\mathbf{A}_{\mathrm{th}}$ [mm^2]	$\mathbf{P}_{\mathrm{ves}}$ [bar]	$\mathbf{V}_{\mathrm{ves}}$ [m^3]	**t** [s]	**ΔM** [kg]
200	200	5	30	266
200	250	3	32	284
200	250	5	54	473
20	200	2	100	86
20	250	1	100	86

and for few hours per year, therefore the initial and maintenance costs are more relevant than operating costs. Moreover, it should be installed in current available spaces within the CREA laboratory and this imposes limits on the size and on the power requirement of the test-rig, which roughly can not exceed 400 kW. Finally, the overall costs for designing and constructing the SCO_2PRI test-rig must be compatible with funding opportunities that are available for fundamental research. According to these peculiarities, three different plant configurations are investigated in the next section.

3. Assessment of the test-rig configurations

Three different test-rig configurations are now considered as possible solutions to realize the exemplary expansions A, B, C and D introduced in the previous section. These are an open-loop, batch operating test-rig and and two closed-loop, continuous operating plants. In the following subsections a brief description and the initial sizing of the main components are reported for each configuration. As a preliminary step, a nozzle throat area of 200 mm^2 was chosen. However, as explained in the following, the flow rate associated to such a relatively large throat area is not compatible with the design constraints and a more realistic throat area of 20 mm^2 is finally chosen.

3.1. Batch operation

The first configuration considered for the SCO_2PRI test-rig consists in the simple open-loop facility sketched in Figure 2. An heated pressurized vessel is filled with CO_2 cylinders up to a pressure greater than the one at the beginning of the expansions. Then, through a control valve, the selected expansion is realized in the nozzle, which discharges into a dump tank equipped with a vacuum pump to set the desired back pressure. Carbon dioxide is eventually released into the atmosphere. This set-up is very similar to the one currently available at MIT [16].

The main advantage of this solution is the simplicity and, thus, the low initial and maintenance costs. On the other hand, the batch operation imposes a limit to the experiment duration, which strictly depends on the volume and initial pressure of the vessel. A target test duration of 100 s is pursued. Table 1 reports the time and the mass released during the expansion B using different vessels and initial pressure, computed through the quasi-1D theory and assuming the process adiabatic. Unfortunately, with the initial nozzle with $A_{\mathrm{th}} = 200$ mm^2, it is possible to perform only short tests, even by using a quite large vessel of 5 m^3. According to these results and to the similar ones obtained for the other expansions but not reported here for brevity the flow rate is reduced by one-tenth so that $A_{\mathrm{th}} = 20$ mm^2. With this geometry, the target test duration can be achieved. A further drawback, inherently related to batch operation,

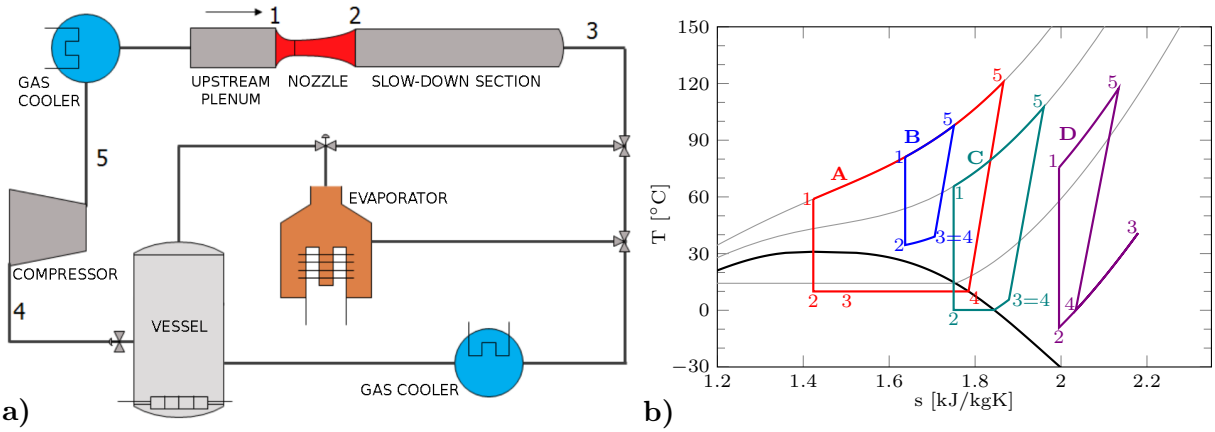

Figure 3: Compressor-based configuration: *a)* sketch of the plant, *b)* exemplary thermodynamic cycles for expansions (1-2) of interest. Points from 1 to 5 identify different steps: 1-2 nozzle expansion, 2-3 slowing down, 3-4 evaporation/cooling, 4-5 compression, 5-1 cooling.

	$\mathbf{P_1}$ [bar]	$\mathbf{T_1}$ [°C]	$\mathbf{P_2}$ [bar]	$\mathbf{T_2}$ [°C]	$\mathbf{T_3}$ [°C]	$\mathbf{T_4}$ [°C]	$\mathbf{T_5}$ [°C]	$\mathbf{W_c}$ [kW]
A	150.0	58.9	45.0	10.0	10.0	10.0	120.8	121.8
B	150.0	81.1	75.0	34.5	39.0	39.0	97.7	64.0
C	100.0	65.6	35.0	0.1	5.6	5.6	107.5	52.2
D	62.1	75.5	34.0	-9.2	40.8	0.0	117.4	33.4

Table 2: Thermodynamic cycles for the four expansions in the "inverse" Joule-Brayton configuration. $\mathbf{W_c}$ is the estimated power required by the compressor for $A_{\text{th}} = 20$ mm^2.

concerns the difficulties in reaching steady state: this requires an accurate and fast control of the throttling valve, because of the emptying of the pressurized vessel and of the filling of the dump tank. The inaccurate control of the thermodynamic state in the steady flow could jeopardize the possibility of using the test-rig in the close proximity of the liquid-vapor critical point and its usage as a pressure probe calibration facility. In conclusion, the analysis of the strengths and limitations of this configuration suggests to discard batch-operation option and to investigate a different solution.

3.2. "Inverse" Joule-Brayton cycle

The first closed-loop configuration can be described as an "inverse" Joule-Brayton cycle, in which a compressor is used to restore the pressure after the nozzle expansion. Since the compressor represents the main (and the most expensive) component of the test-rig, the compressor is sized first. For simplicity, a single machine that permits to realize all expansions is preferred. For this reason, the limit temperatures $T_{\text{min}} = 0$°C and $T_{\text{max}} = 120$°C are imposed for the suction and discharge sections, respectively, and the end states of expansions A, C and D are chosen according to them. Moreover, for expansion A, a pressure $P_2 = 45$ bar is imposed to avoid excessively large compression and cooling power, while for expansion D, a gas cooler is added to reduce the inlet (and so the outlet) temperature of the compressor. Figure 3 displays the sketch of the plant along with the thermodynamic cycles in the T-s plane, which are detailed in Table 2. The table also reports the estimates of the electrical power consumption, computed assuming an isentropic efficiency $\eta = 0.6$ for the compressor and neglecting all other losses, for the reduced throat area. For the initial area $A_{\text{th}} = 200$ mm^2, the power required by the compressor considerably exceeds the available one.

The preliminary computations allow to define the operating range of the required compressor,

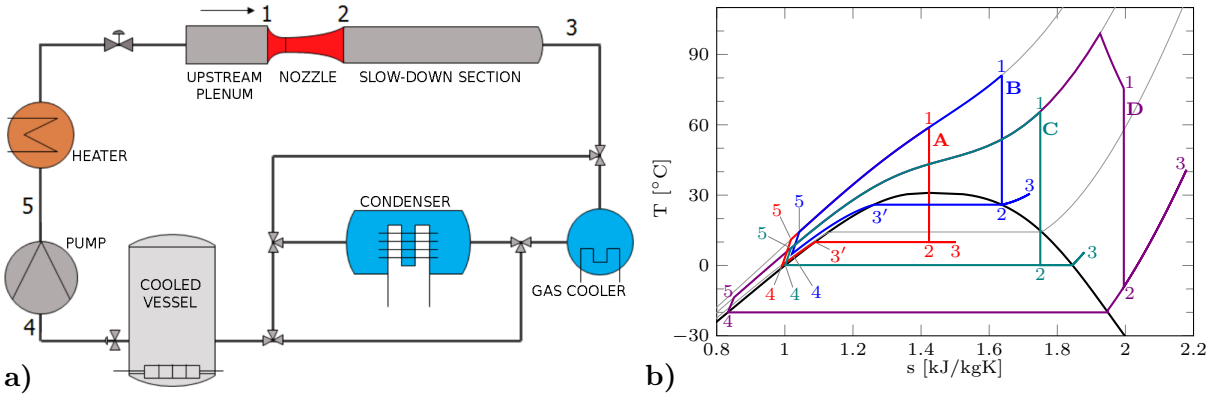

Figure 4: Pump-based configuration: *a)* sketch of the plant, *b)* exemplary thermodynamic cycles. Points from 1 to 5 identify different steps: 1-2 nozzle expansion, 2-3 slowing down, 3-4 de-superheating/condensation/cooling, 4-5 compression, 5-1 heating. For tests A and B, 3′-4 indicates the additional cooling to avoid cavitation issues.

	$\mathbf{P_4}$ [bar]	$\mathbf{T_4}$ [°C]	$\mathbf{T_5}$ [°C]	$\mathbf{W_p}$ [kW]	$\dot{\mathbf{Q}}_\mathbf{h}$ [kW]	$\dot{\mathbf{Q}}_\mathbf{c}$ [kW]	$\mathbf{W_c}$ [kW]	$\dot{\mathbf{m}}$ [kg/s]
A	45.0	0.0	11.1	29	200	229	65	1.59
B	65.7	5.0	14.3	17	221	239	68	1.16
C	35.0	0.2	7.4	8	159	167	88	0.7
D	20.0	-20	-13.6	5	120	125	94	0.36

Table 3: Thermodynamic cycles in the Rankine configuration, with $A_{\text{th}} = 20$ mm^2. $\mathbf{W_p}$ and $\mathbf{W_c}$ are the electrical powers required by the pump and the chiller unit, $\dot{\mathbf{Q}}_\mathbf{h}$ and $\dot{\mathbf{Q}}_\mathbf{c}$ are the thermal powers exchanged in the heating and cooling sections.

which is found to be a volumetric one, and to proceed with the selection of the machinery among the commercial available solutions. The machinery design is commissioned to a specialized company, which proposes an ad hoc reciprocating compressor, which a particular massive structure, since the high densities reached by the CO_2 in the specific operating conditions generate considerable axial stresses. The resulting compressor size is much larger than the one usually required by similar pressure ratios, flow rates and powers in a standard thermodynamic region, i.e. far from the critical point. Therefore, this extremely large (and noisy) machinery cannot be installed at the laboratory. Furthermore, the purchase of this component only would exhaust almost all the initial available fund. For these reasons, compressor-based test-rig is not deemed to be adequate.

3.3. Rankine cycle

A pump-based plant is now considered for the SCO_2PRI test-rig. This configuration results in a transcritical Rankine cycle with phase transition, as sketched in Figure 4. After the nozzle expansion and the subsequent deceleration, the flow is condensed and liquid CO_2 is pumped to the inlet nozzle pressure, then it is heated until the required temperature. The imposed nozzle exit states are the same used for the previous configurations (i.e. points 1, 2 and 3 in Table 2), except that expansion B has been extended until the VLE curve to make condensation possible ($T_2 = 25.9$°C). To realize expansion D, the pressure at the exit of the pump must be higher than the critical one, and a throttling process is performed before entering the nozzle to reach the correct pressure. All thermodynamic cycles are shown in Figure 4; relevant data are reported in Table 3.

First, the pump is characterized. As expected, the power consumptions, reported in Table 3 and computed assuming an isentropic efficiency $\eta = 0.6$, are much smaller than the ones

computed for the compressor. Indeed, the specific enthalpy drop in the liquid region is smaller than the one in the gas region for the same pressure ratio. From a preliminary analysis, a volumetric pump is needed. With this regards, possible problems may occur due to the relatively high compressibility of sCO_2 with respect to standard liquids, especially in test A and B. For this reason, in these two cycles, an additional cooling is performed at the end of the condensation to reach a lower pump inlet temperature, and therefore reducing the liquid compressibility.

Differently from the "inverse" Brayton cycle, the heating and cooling processes are relevant both from the technical and the economic point of view, therefore a preliminary assessment of the test-rig configuration has to include them. Table 3 reports also the heating and cooling powers (included de-superheating and condensation). The results are reported only for the nozzle with $A_{\text{th}} = 20$ mm^2 because the available power is not sufficient if the larger area of $A_{\text{th}} = 200$ mm^2 is considered.

Despite the quite large thermal power involved, relatively standard components can be used to perform the required processes and no particular technical problems are expected in this regard. From a first estimate on the basis of the commercial available components similar to the ones required by this plant, the space required to house all the parts of the test rig is congruous with the laboratory capacity. Therefore, a more accurate investigation and a preliminary design of the components of the pump-based configuration are performed. As final remark, a further advantage provided by a phase-transition configuration concerns the possibility of carrying out research using different fluid phases, such as liquid or two-phase flows of CO_2.

4. Preliminary design of the SCO_2PRI test-rig

The previous analysis of the candidate plant configurations led to the selection of the pump-based closed-loop Rankine cycle. This section presents a preliminary design of the main components and of the test section of the SCO_2PRI. The components are selected among commercially available (possibly customized) solutions with the primary aim of realizing all four expansions by means of the same balance of plant. In this respect, it should be clarified that the different expansions will be investigated in separate experimental campaigns, therefore the possibility of connecting the different cycles is not required. For what concerns the test section, four different nozzles are designed and a modular solution is adopted so that they can be installed within the same arrangement.

4.1. Analysis of test-rig components

The first component that is analyzed is the pumping section. Since the flow rates in the four tests are rather different, a parallel configuration that includes two pumping groups working at constant speed is adopted and one device can be excluded through a by-pass valve. Each pumping group is composed by a plunger pump that has a maximum discharge pressure of 150 bar and a maximum inlet pressure of 65 bar, a 18.5 kW electrical motor, a pulsation damper and other safety accessories.

The heating section is now detailed. The temperature of the sCO_2 flow is increased by means of an heater exchanger that is fed on the hot-side by a thermal oil flow from a mono-bloc gas heater, already equipped with control and safety equipments. Plate & Shell Heat Exchangers (PSHE) are exploited to obtain benefits in terms of compactness and heat transfer efficiency at the operating temperatures and pressures. More specifically, a fully welded pack of circular plates of stainless steel with a thickness of 1.5 mm is contained in a carbon steel shell of approximately 0.13 m^3. Thanks to the peculiar design realized by a specialized company, this kind of heat exchangers can safely operate up to 170 bar. The issue of dealing with different flow rates and different inlet/outlet temperatures is solved by dimensioning all components on the most demanding case, e.g. test B. Since the described device cannot guarantee fine control of the

sCO_2 temperature at the nozzle inlet, which is of paramount important for expansion A, a 2 kW electrical heater is added before the nozzle for control purposes.

For the cooling section, the use of a chiller is mandatory due to the low temperatures. A direct cooling process with a chiller unit specially designed for the SCO_2PRI test-rig is used to perform de-superheating, condensation and sub-cooling processes, depending on the performed test. This technical solution requires the design of an additional cycle for the refrigerant fluid which, according to the required tasks and operating conditions, is ammonia. The design choice consists in the standard, widely-used single-stage vapor-compressor cycle, which is composed by a compressor, a condensing section, an expansion valve and an evaporator. The two main steps of the design process concern the definition of the condensation and evaporation temperatures, while the design of the refrigerant cycle is commissioned to a specialized supplier. The condensation temperature is set at 38°C and a water-cooled condenser is used to exploit a cooling tower already available at the laboratory. For the evaporation temperature, different values are established according to the test: for test A, B and C, a temperature difference of $10 - 15$°C is imposed between the two fluids; while in test D this difference is reduced to 2°C. The heat required by CO_2 de-superheating and condensation is absorbed by ammonia through a PSHE with a design thermal power of 400 kW, while a smaller dry expansion evaporator (design power of 50 kW) accounts for the additional cooling required in test A and B.

Finally, after a preliminary sizing of the SCO_2PRI plant, including also piping, the mass of CO_2 circulating within the plant is estimated. This quantity varies between 57 and 78 kg, depending on the considered test. Therefore, an accumulation tank of 50 L is included in the plant for storage purposes. Accounting also for this vessel, the area required to place all components is estimated to be less than 15 m^2. Moreover, the thermal oil heather and the chiller unit, which result to be the largest parts, can be safely placed in an external area adjacent to the laboratory.

4.2. Design of the test section

The test section, which includes the nozzle along with the downstream slow-down section, is now detailed. In particular, the geometry of the nozzles delivering the desired expansion ratios at the diverse operating conditions is designed. Since the exemplary supersonic expansions are defined considering chocked flows, four different convergent-divergent nozzles are required.

Before the detailed design of the geometry, the flow inside the nozzle is investigated more thoroughly. Figure 5 shows the variation of the Mach number with the density during all expansions, computed according to the quasi-1D theory for isentropic flows. The NIST databse REFPROP [27] is exploited to perform the thermodynamic evaluations by using the reference equation of state of Span and Wagner [13]. As expected, a non-monotone variation occurs during the test A. This behavior is typical of fluids characterized by a value of the fundamental derivative of gas-dynamics Γ between zero and one and it is related to close-to-critical-point effects. Expansions B, C and D lies in the thermodynamic region where $\Gamma > 1$ and the Mach number is monotonically increasing to supersonic values, similarly to what observed in the ideal flows of dilute gases. However, non-ideal compressible-fluid effects are relevant—including the non-ideal dependence of the sound speed on the density in isothermal transformations—and strongly influence the dynamics of the fluid in expansions B, C and D as well.

For the nozzle geometry design, a rectangular cross-section is adopted to produce a two-dimensional flow and to perform flow visualization more easily. With this regards, one wall of the test section consists in a planar glass windows. Since the throat of the nozzle is chocked, the thermodynamic state there is completely defined. Thus, the geometry of the nozzle can be computed in two independent steps. First, the methods of characteristics [28] is used to compute the length and the shape of the divergent section, in order to obtain an uniform flow at the exit with velocity parallel to the nozzle axis and the design pressure ratio. The state-of-the-art multi-

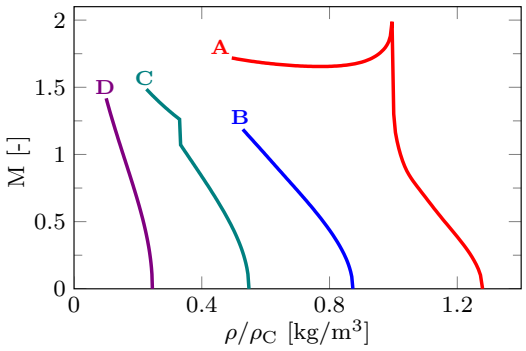

Figure 5: Variation of Mach number with density in the four exemplary expansions depicted in Figure 4. Density is scaled with respect to the critical value. As expected, a non-monotone variation occurs during Expansion A, where Γ is below 1.

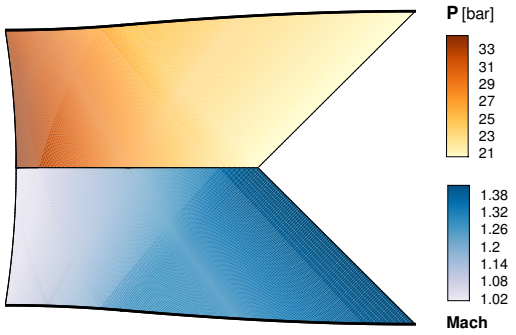

Figure 6: Divergent part of the nozzle for expansion D. Pressure and Mach contour plot computed by means of the method of characteristics, with the multi-parameter equation of state [13], are shown.

parameter thermodynamic model for CO_2 proposed in [13] is used. Additional details about the design procedure including code validation can be found in [29, 30]. Figure 6 displays the results obtained for test D, both in terms of pressure and Mach distribution. Then, the convergent part can be designed. Since this part of the geometry has a limited influence on the flow downstream the chocked throat, a polynomial profile is designed to realize the gradual area variation from the inlet section to the throat. To enhance flow regularity, the first and second derivatives of the divergent profile are matched at the throat. As a final remark, it should be pointed out that the geometry here presented refers to the inviscid core of the nozzle flow, thus additional CFD simulations will be performed to accurately predict the boundary layer in a further step of the plant design process.

5. Discussion and conclusions

Despite the wide use of sCO_2 in energy and chemical industry, the knowledge about carbon dioxide behavior in the supercritical region and near the critical point is still deficient, both in terms of fundamentals and of experimental data required for validation. In order to contribute to fill this lack, a new test-rig, named SCO_2PRI, is under-design at CREA Laboratory of Politecnico di Milano.

Within the non-ideal compressible fluid dynamics region, four different supersonic expansions through a convergent-divergent nozzle have been defined and different plant configurations have been taken into consideration to realize them. Due to the flow rates and the necessity of performing steady measurements, a closed-loop continuous-operating plant has been preferred. Moreover, the initial desired throat area had to be scaled to comply with the power availability of the laboratory. The "inverse" Joule-Brayton solution revealed to be inadequate due to the size and cost of the volumetric compressor, which has to operate in a region where the fluid density has high values, resulting in high stresses on the piston. Thus, the pump-based Rankine cycle configuration has been analyzed and it resulted to be feasible according to the economic and logistic constraints. Moreover, the choice of the Rankine cycle configuration results in a more flexible plant layout, which allows also for investigating the fluid flow at different conditions, including liquid and two-phase.

Similarly to the standard Rankine cycle, the main components of the SCO_2PRI test-rig are a pumping group, a heating section, the test section (expander) and the cooling section. The

availability of these components has been verified from suppliers and customized solutions have been designed when they were not commercially available. The pumping section is composed by two volumetric pumps which can operate independently to deal with the different flow rates that characterize the four expansions. On the contrary, heat exchangers in the heating and cooling sections have been sized on the most demanding case. An auxiliary cycle for the refrigerant (i.e. ammonia) was designed which includes a chiller. The chiller unit resulted to be the most expensive component in the test-rig, because of the low temperatures to be reached in evaporators. However, since low temperatures (less than 0°C) are required only in test conditions D, the feasibility of a less expensive test-rig in which only the chiller is sized on the three less demanding test cases was assessed. Such a pilot plant includes all the original components, except that the chiller unit that has been replaced by a smaller commercial available one.

In conclusion, the feasibility of the SCO_2PRI test-rig has been assessed for diverse test conditions and against different experimental techniques, including flow visualization and pneumatic measurements of non-ideal compressible fluid dynamics. The measurements of thermodynamic quantities along an expansion through the critical point, where non-monotone variation of the Mach number with density is expected, would supply important information that could fill the gap in sCO_2 fundamental knowledge. Future research activities will concern the design of all the other components of the test-rig, as well as dynamic simulations of its operation, including filling and starting. Moreover, the control and measurements systems will be detailed and designed.

References

[1] Angelino G 1969 *ASME Journal of Engineering for Power* **10** 272
[2] Feher E 1968 *Energy conversion* **8** 85–90
[3] Mahaffey J, Kalra A, Anderson M and Sridharan K 2014 *Supercritical CO2 Power Cycles Symp.*
[4] Ahn Y, Bae S J, Kim M, Cho S K, Baik S, Lee J I and Cha J E 2015 *Nucl. Eng. Technol.* **47** 647 – 661
[5] Reverchon E and Pallado P 1996 *J. of Supercritical Fluids* **9** 216–221
[6] Subramaniam B, Rajewski R A and Snavely K 1997 *J. Pharm. Sci.* **86** 885–890
[7] Sun X Y, Wang T J, Wang Z W and Jin Y 2002 *J. of Supercritical Fluids* **24** 231–237 ISSN 08968446
[8] Ito T, Otani Y and Inomata H 2004 *Sep. Purif. Technol.* **40** 41–46
[9] Zienkiewicz H K and Johannesen N H 2006 *J. Fluid Mech.* **17** 499
[10] Griffith W C and Kenny A 2006 *J. Fluid Mech.* **3** 286 ISSN 0022-1120
[11] Michels A, Sengers J V and van der Gulik P S 1962 *Physica* **28** 1216–1237
[12] Kim J K and Aihara T 1992 *International journal of heat and mass transfer* **35** 2515–2526
[13] Span R and Wagner W 1996 *J. Phys. Chem. Ref. Data* **25** 1509–1596
[14] Baltadjiev N, Lettieri C and Spakovszky Z 2014 *ASME Turbo Expo* **137** ISSN 0889-504X
[15] Rinaldi E, Pecnik R and Colonna P 2015 *J. Eng. Gas Turbines Power* **137** 1–7
[16] Lettieri C, Yang D and Spakovszky Z 2014 *Supercritical CO2 Power Cycles Symp.*
[17] Lee J, Cho S, Cha J and Lee J 2016 *Supercritical CO2 Power Cycles Symp.*
[18] Sánchez D, Monje B, Chacartegui R, Barragán J, Pajuelo E, Gómez J and Sánchez T 2013 *ASME Turbo Expo* (San Antonio, USA)
[19] Conboy T, Wright S, Pasch J, Fleming D, Rochau G and Fuller R 2012 *ASME Turbo Expo* pp 941–952
[20] Clementoni E, Cox T and Sprague C 2014 *J. Eng. Gas Turbines Power* **136** 1–6
[21] Moore J, Brun K, Evans N and Kalra C 2015 *ASME Turbo Expo*
[22] Rochau G E, Drennen T, Pasch J, Fleming D, Carlson M, Dawson L, Kruizenga A and Brooks R 2016 *Supercritical CO2 Power Cycles Symp.*
[23] Liao S M and Zhao T S 2002 *Journal of Heat Transfer* **124** 413–420
[24] Shiferaw D, Montero Carrero J and Le Pierres R 2016 *Supercritical CO2 Power Cycles Symp.*
[25] Callen H B 1985 *Thermodynamics and an introduction to thermostatistics* Second ed (Wiley)
[26] Thompson P A 1972 *Compressible-Fluid Dynamics* (McGraw-Hill Inc.)
[27] Lemmon E W, Huber M L and McLinden M O NIST Reference Fluid Thermodynamic and Transport Properties – REFPROP National Institute of Standards and Technology, Boulder, Colorado
[28] Zucrow M H and Hoffman J D 1976 *Gas dynamics* vol 1 (Wiley, Jhon & Son)
[29] Guardone A 2010 *7th HEFAT Conference* (Turkey)
[30] Guardone A, Spinelli A and Dossena V 2013 *J. Eng. Gas Turb. Power* **135** 042307–1